RSC Advances

PAPER

View Article Online
View Journal | View Issue

Cite this: *RSC Adv.*, 2025, **15**, 25510

Eradication of MRSA biofilms using amphiphilic cationic coumarin derivatives†

Samuel O. Nitschke,[a] Muhammed Awad,[ab] Alysha G. Elliott,[c] Gabrielle Lowe,[c] Chris Leigh,[d] Ken Neubauer,[d] Nicky Thomas,[a] Shane M. Hickey *[a] and Sally E. Plush *[a]

Received 19th June 2025
Accepted 10th July 2025

DOI: 10.1039/d5ra04358a

rsc.li/rsc-advances

Amphiphilic coumarin derivatives have demonstrated potent antibiofilm activity against established methicillin-resistant *Staphylococcus aureus* (MRSA) biofilms. Scanning electron microscopy (SEM) revealed morphological changes to bacterial cells and eradication of extracellular matrix from established MRSA biofilms when treated with 7-benzyloxy coumarin derivatives.

An estimated 1.27 million deaths were directly caused by antimicrobial resistant bacterial infections in 2019.[1] One of the most prolific drug-resistant bacterial pathogens is methicillin-resistant *Staphylococcus aureus* (MRSA). MRSA is a leading cause of nosocomial wound infections and is associated with significant morbidity and mortality.[2] Treatment of MRSA infections is complicated by their tendency to form biofilms, which are implicated in approximately 80% of all bacterial infections in humans.[3] Bacteria residing within biofilms are less susceptible to antibiotics, host immune defences, disinfectants, and environmental stressors, compared to planktonic cells.[4] This increased tolerance is partly attributed to the complex extracellular matrix of biofilms that acts as a physical barrier; bacteria residing within a biofilm environment are 100–1000× more tolerant to antibiotics compared to planktonic cells.[5] Cellular populations within biofilms are also heterogeneous, consisting of metabolically active and metabolically silent (persister) cells, which are more tolerant of antibacterial treatments.[6] Moreover, cellular interactions within the biofilm environment allow the transfer of antimicrobial resistance genes.[7] Taken together, the effective treatment of MRSA is significantly complicated by biofilm formation that imposes both physical and chemical barriers to overcome.[8,9] Therefore, antibacterial agents that can penetrate and eradicate bacterial biofilms are highly desirable therapeutics in modern medicine.[10–12]

Cationic antimicrobial peptides (CAMPs) are one of the first lines of defence against invasive microbial infections in humans.[13] This family of molecules are typified by an amphiphilic topology—well-defined cationic and hydrophobic regions—which is thought to be critical to their antibacterial activity.[14] Due to their membrane-active mechanism of action, CAMPs can kill bacteria regardless of their metabolic state[15] and have shown a decreased propensity to elicit the formation of resistance.[16] CAMPs have shown promise as antibiofilm agents, and have demonstrated the ability to eradicate established bacterial biofilms.[17] Unfortunately the clinical deployment of CAMPs has been hindered by several factors including the high costs associated with manufacture, susceptibility to proteolysis, and poor toxicity profiles.[18] To overcome these limitations, synthetic CAMP mimetics have been explored as novel antibacterial agents,[19] as they offer the potential to decrease manufacturing costs[20] and are typically more stable in biological environments.[21] Small-molecule CAMP mimetics frequently rely on a rigid scaffold to confer amphiphilic topology, with organic frameworks such as norbornane,[22–24] triazine,[25] xanthone,[26] and coumarin[27,28] having been reported in the literature.

In this work, a 4-methylumbelliferone scaffold was selected to build a novel series of structurally amphiphilic compounds, with distinct cationic and hydrophobic groups installed at the 3- and 7-positions, respectively. The compounds featured either a charged amine (**1** and **2**, Fig. 1) or a charged guanidine derivative (**3–5**) headgroup to mimic lysine and arginine residues in CAMPs, respectively.

Guanidines have been proposed to improve membrane interactions due to the ability to form bidentate hydrogen

[a]*Clinical and Health Sciences, University of South Australia, Adelaide, South Australia, 5000, Australia. E-mail: sally.plush@unisa.edu.au*

[b]*Basil Hetzel Institute for Translational Health Research, Woodville, South Australia, 5011, Australia*

[c]*Institute for Molecular Bioscience, The University of Queensland, Brisbane, Queensland, 4072, Australia*

[d]*Adelaide Microscopy, The University of Adelaide, Adelaide, South Australia, 5000, Australia*

† Electronic supplementary information (ESI) available: Methods and data for physicochemical characterisation (Log *P* and DLS); methods and data for the antibacterial and toxicity screening performed by CO-ADD; methods and data for antibiofilm evaluation (crystal violet and MBEC); methods for SEM imaging of MRSA biofilms; compound synthesis; NMR (^{1}H, ^{13}C, HSQC, and HMBC) spectra of all compounds; HRMS spectra of all coumarin compounds; RP-HPLC chromatograms of all coumarin compounds; ^{1}H NMR stability data for compound **4**. See DOI: https://doi.org/10.1039/d5ra04358a

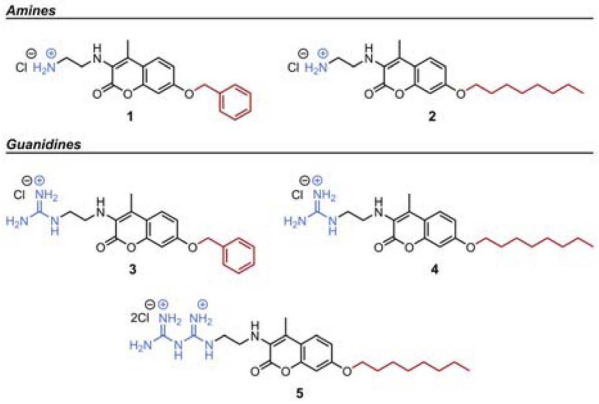

Fig. 1 Coumarin amines (**1** and **2**) and coumarin guanidines (**3**, **4**, and **5**).

bonds with anionic phospholipids located on the bacterial membrane.[29] The biguanide moiety was also included in this study given the work of Rahn *et al.*,[30] who reported biguanide-functionalised vancomycin derivatives that exhibited broad-spectrum antibacterial and antibiofilm activity. Two hydrophobic groups (benzyl and *n*-octyl) were included in the design of the coumarin amphiphiles targeted in this study. A benzyl group was considered as an analogue of phenylalanine, which typically imparts a lipophilic character to CAMPs.[31] The inclusion of an *n*-octyl hydrophobic tail is justified by the work of van Groesen[32] and Mingeot-Leclercq,[33] who have accessed *n*-alkylated derivatives of well-known antibiotics such as vancomycin and neomycin, respectively. In their work, the inclusion of *n*-alkyl hydrophobic groups imparted an increase in the potency of the antibiotics and broadened their activity spectrum to effect both Gram-positive and Gram-negative bacteria.[32,33] In total, five compounds were synthesised that contained either a benzyl (**1** and **3**) or an *n*-octyl (**2**, **4**, and **5**) hydrophobic tail with a primary amine (**1** and **2**) or guanidine-based (**3**, **4**, and **5**) cationic headgroup (Fig. 1). The multistep synthesis of these coumarin compounds is depicted in Scheme S1 (ESI†).

To first assess the antibacterial activity of the coumarin amphiphiles, all compounds were screened against a panel of pathogenic Gram-positive and Gram-negative bacterial strains (Table S3, ESI†). A micro-broth dilution assay was used to determine the minimum inhibitory concentration (MIC) of the compounds against planktonic bacteria with the highest concentration tested being 32 μg mL^{-1}. In all instances, activity was most prominent against Gram-positive MRSA, with some activity observed against Gram-negative strains. Octyl coumarins outperformed their benzyl counterparts for both the amine and guanidine series. For the amine coumarins, benzyl **1** demonstrated an MIC of 32 μg mL^{-1} against MRSA, whilst an MIC of 2 μg mL^{-1} was recorded for octyl **2**. For the guanidine coumarins, an MIC of 16 μg mL^{-1} was recorded for benzyl **3** compared to an MIC of 8 μg mL^{-1} for octyl **4**. Modification of the guanidine moiety resulted in improved potency against MRSA with biguanide **5** exhibiting an MIC of 4 μg mL^{-1}.

The improved activity of the octyl coumarins compared to the benzyl derivatives can be attributed to the increase in relative lipophilicity of the molecules. Previous studies have used *in silico* modelling to demonstrate the ability of similarly designed peptidomimetic amphiphiles to aggregate and perturb the bacterial membrane.[34] As such, the six coumarin amphiphiles reported in this study were evaluated for their propensity to aggregate in an aqueous environment using dynamic light scattering (DLS, Table S1 and Fig. S3, ESI†). The calculated *Z*-average diameters and PDIs indicated that these molecules readily aggregate in an aqueous environment that is likely fundamental to their antimicrobial activity, in accordance with related literature examples.[34,35] Moreover, previous reports are suggestive that an optimal hydrophobic window exists for amphiphilic compounds with respect to antimicrobial activity; if the molecule is too hydrophilic then it typically offers no activity, whilst if a molecule is too hydrophobic it imparts toxicity against mammalian cell lines as well as the targeted pathogen.[36] The *c*log *P* values were calculated for all compounds (Table S1, ESI†) after validating the accuracy of the predictive software by experimentally determining the log *P* values for 7-benzyloxy guanidine **3** at three different concentrations (Table S2, Fig. S1 and S2, ESI†). The *c*log *P* values for all coumarin analogues were dictated by hydrophobic portion of the molecule, with derivatives bearing a benzyl group at the 7-position (**1** and **3**) approximately 1 log unit lower than the derivatives furnished with an octyl chain in this position (**2**, **4**, and **5**).

To assess the ability of our small series of cationic coumarin amphiphiles to impact biofilm communities, established MRSA ATCC 43300 biofilms were treated with each compound and biofilm reduction was measured using a crystal violet assay.[37] Initial screening of antibiofilm activity involved treating MRSA biofilms with coumarin amphiphiles at concentrations approximately 10× their respective MICs against planktonic MRSA, to account for the increased resistance of biofilm bacteria (Fig. 2A and Table S5, ESI†).[38] Both benzyl coumarins (**1** and **3**) were found to decrease the mass of MRSA biofilms by over 70% ($p \leq 0.0001$). Significant biofilm mass reduction ($p \leq 0.01$) was also observed for guanidine **4** (>40%), whilst no activity was observed for biguanide **5**. Given the promising antibiofilm activity observed across the series of coumarin compounds at these concentrations, the compounds were subsequently tested at equivalent concentrations (Fig. 2B). In this second round of screening, only antibiofilm activity for the two benzyl coumarins (amine **1** and guanidine **3**) was observed. To probe the dose-dependent antibiofilm activity of the benzyl coumarins, MRSA biofilms were treated over a concentration range of 32–256 μg mL^{-1} (Fig. 2C and D).

Both benzyl coumarins (**1** and **3**) caused a dose-dependent reduction in biofilm mass, reaching 60% and 70% biofilm eradication at 128–256 μg mL^{-1}, respectively, with no significant difference between the two concentrations ($p > 0.05$). In addition, the minimum biofilm eradication concentration (MBEC) of benzyl coumarin **1** was determined using recovery methods (Table S9 and Fig. S4, ESI†). Following treatment of MRSA biofilms with **1** at 128 μg mL^{-1}, significant killing of MRSA was observed ($p \leq 0.0001$). At 128 μg mL^{-1}, **1** caused a 5-log reduction in viable bacterial cells, and at 256 μg mL^{-1}, **1** was

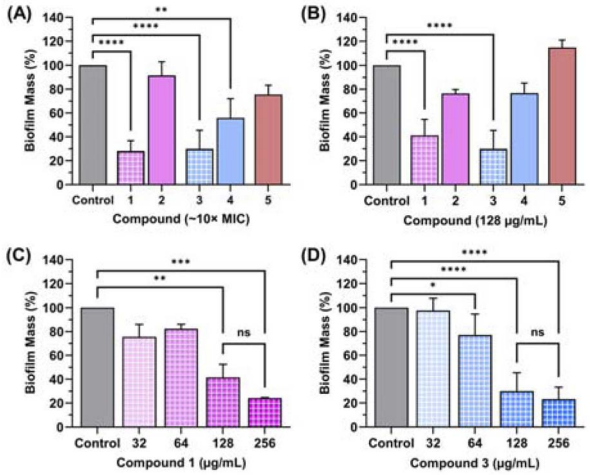

Fig. 2 Mass reduction of methicillin-resistant *S. aureus* (MRSA) biofilms when treated with coumarin amphiphiles **1** (pink squares), **2** (pink), **3** (blue squares), **4** (blue), and **5** (red) for 24 h. (A) MRSA biofilm mass reduction at ~10× MIC values. (B) MRSA biofilm mass reduction at 128 μg mL^{-1} (C) MRSA biofilm mass reduction for compound **1** (32–256 μg mL^{-1}). (D) MRSA biofilm mass reduction for compound **3** (32–256 μg mL^{-1}). Data presented as mean ± SD of 6 technical replicates and 3 biological replicates. * = $p \leq 0.05$, ** = $p \leq 0.01$, *** = $p \leq 0.001$, **** = $p \leq 0.0001$. Checkered patterning corresponds to coumarins with a benzyl tail and solid patterning corresponds to coumarins with an octyl tail.

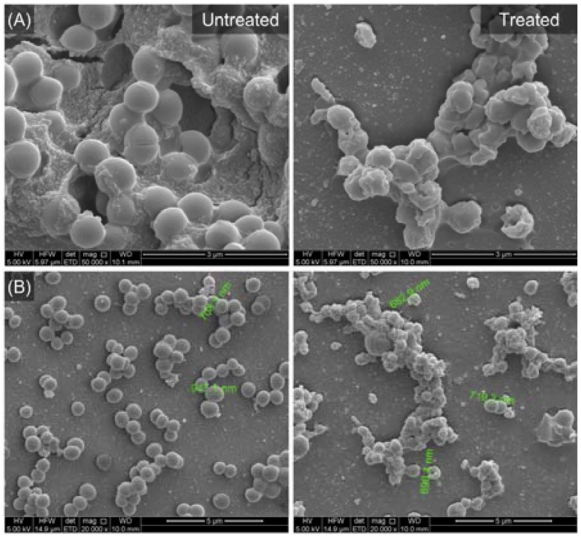

Fig. 3 Scanning electron microscopy (SEM) micrographs of methicillin-resistant *S. aureus* (MRSA) biofilms: untreated (left) and treated with 128 μg mL^{-1} of benzyl coumarin **1** for 24 h (right). (A) Images showing loss of extracellular matrix between untreated and treated samples (50 000× magnification). (B) Images showing change in cell size between untreated and treated samples (20 000× magnification).

bactericidal, causing 99.9% eradication of bacteria with no significant difference between the two concentrations ($p > 0.05$). Together, these results suggest the benzyl moiety at the 7-position of the coumarin scaffold is a key driver of antibiofilm activity.

To further investigate the biofilm disruption caused by the benzyl coumarins, MRSA biofilm morphology was investigated using scanning electron microscopy (SEM). Treatment of MRSA biofilms with benzyl coumarin **1** caused changes in extracellular matrix, colony, and cellular morphology (Fig. 3). The main difference between untreated and treated biofilms was the dispersion of cellular clusters that were embedded in the extracellular matrix, indicating that treatment caused matrix dissolution (Fig. 3A). In addition, bacterial cells in the treated samples showed a marked change in cellular shape, with most cells displaying a shrunken and rough cellular surface indicative of cell death[39] instead of a smooth surface, as depicted in the untreated biofilm. Cell size was also affected, with cells in the treated biofilm having a smaller average size (698 nm, Fig. 3B) compared to cells in the untreated biofilm (828 nm).

Coumarin amphiphiles were also assessed for mammalian cytotoxicity against HEK-293 cells and red blood cells (RBCs), as measured using the respective CC_{50} and HC_{10} values (Table S4, ESI†). Both amine coumarins (**1** and **2**) exhibited significant cytotoxicity against HEK-293 cells with CC_{50} values of 7.1 μg mL^{-1} and 4.7 μg mL^{-1}, respectively. Comparatively, guanidine coumarins exhibited improved mammalian cytotoxicity profiles, with benzyl coumarin **3** exhibiting no significant activity at 32 μg mL^{-1}. Haemolytic activity differed between benzyl and octyl derivatives; all octyl coumarins exhibited significant haemolytic activity, however, both benzyl coumarins (**1** and **3**) exhibited a more favourable haemolytic profile (HC_{10} > 32 μg mL^{-1}). These results suggest that the benzyl coumarins, particularly guanidine coumarin **3**, may elicit antibacterial activity in a different manner to octyl derivatives.

In the current study, five cationic coumarin amphiphiles were designed, synthesised, and evaluated for their antibacterial activity against planktonic bacteria and MRSA biofilms. Crystal violet assays revealed that benzyl coumarins were capable of eradicating MRSA biofilms at < 4× MIC values. Benzyl coumarin **1** decreased biofilm mass by solubilising the extracellular matrix and caused deformation of MRSA biofilms at a structural and cellular level. SEM revealed morphological changes in the biofilm extracellular architecture following treatment. The two benzyl derivatives that displayed antibiofilm activity (**1** and **3**) were non-haemolytic and benzyl coumarin **3** was also non-toxic against HEK-293 cells. Although the much higher concentrations required for antibiofilm activity would likely limit their use in a clinical setting due to toxicity concerns, this work represents an important contribution to the field that can be built upon in the pursuit of much needed new antibiofilm and biofilm-sensitising agents.

Data availability

The data supporting this article have been included as part of the ESI.† The NMR spectral data for the synthesised compounds are available on figshare at **https://doi.org/10.6084/m9.figshare.28340399.v3**. FID files are numbered according to the compound numbers in the manuscript and ESI,† experiments are numbered according to the following: 1 (^{1}H NMR), 2 (^{13}C NMR), 3 (HSQC), and 4 (HMBC).

Conflicts of interest

There are no conflicts to declare.

Acknowledgements

The antimicrobial toxicity screening performed by CO-ADD (The Community for Antimicrobial Drug Discovery) was funded by the Wellcome Trust (UK) and The University of Queensland (Australia). Bacterial and human cell lines were acquired from the America Type Culture Collection (ATCC). The authors acknowledge the instruments and expertise of Microscopy Australia at Adelaide Microscopy, The University of Adelaide, enabled by NCRIS, university, and state government support. This work was supported by the Australian Government Research Training Program domestic (RTPd) Scholarship and the University of South Australia Post Graduate Award (USAPA) Scholarship.

Notes and references

1 C. J. L. Murray, K. S. Ikuta, F. Sharara, L. Swetschinski, G. R. Aguilar, A. Gray, C. Han, C. Bisignano, P. Rao and E. Wool, *Lancet*, 2022, **399**, 629–655.
2 A. S. Lee, H. de Lencastre, J. Garau, J. Kluytmans, S. Malhotra-Kumar, A. Peschel and S. Harbarth, *Nat. Rev. Dis. Primers*, 2018, **4**, 18033.
3 D. Sharma, L. Misba and A. U. Khan, *Antimicrob. Resist. Infect. Control*, 2019, **8**, 76.
4 O. Ciofu, C. Moser, P. Ø. Jensen and N. Høiby, *Nat. Rev. Microbiol.*, 2022, **20**, 621–635.
5 G. V. Tetz, N. K. Artemenko and V. V. Tetz, *Antimicrob. Agents Chemother.*, 2009, **53**, 1204–1209.
6 B. P. Conlon, *Bioessays*, 2014, **36**, 991–996.
7 C. Uruén, G. Chopo-Escuin, J. Tommassen, R. C. Mainar-Jaime and J. Arenas, *Antibiotics*, 2021, **10**, 3.
8 O. Ciofu, C. Moser, P. O. Jensen and N. Hoiby, *Nat. Rev. Microbiol.*, 2022, **20**, 621–635.
9 H. Van Acker and T. Coenye, *J. Biol. Chem.*, 2016, **291**, 12565–12572.
10 Z. Si, W. Zheng, D. Prananty, J. Li, C. H. Koh, E. T. Kang, K. Pethe and M. B. Chan-Park, *Chem. Sci.*, 2022, **13**, 345–364.
11 N. Raheem and S. K. Straus, *Front. Microbiol.*, 2019, **10**, 2866.
12 J. Hoque, M. M. Konai, S. S. Sequeira, S. Samaddar and J. Haldar, *J. Med. Chem.*, 2016, **59**, 10750–10762.
13 J. Lei, L. C. Sun, S. Y. Huang, C. H. Zhu, P. Li, J. He, V. Mackey, D. H. Coy and Q. Y. He, *Am. J. Transl. Res.*, 2019, **11**, 3919–3931.
14 N. Chen and C. Jiang, *Eur. J. Med. Chem.*, 2023, **255**, 115377.
15 G. Batoni, G. Maisetta and S. Esin, *Biochim. Biophys. Acta Biomembr.*, 2016, **1858**, 1044–1060.
16 A. Peschel and H. G. Sahl, *Nat. Rev. Microbiol.*, 2006, **4**, 529–536.
17 A. D. Verderosa, M. Totsika and K. E. Fairfull-Smith, *Front. Chem.*, 2019, **7**, 824.
18 H. B. Koo and J. Seo, *Pept. Sci.*, 2019, **111**, e24122.
19 C. Ghosh and J. Haldar, *ChemMedChem*, 2015, **10**, 1606–1624.
20 A. K. Marr, W. J. Gooderham and R. E. Hancock, *Curr. Opin. Pharmacol.*, 2006, **6**, 468–472.
21 S. Rotem and A. Mor, *Biochim. Biophys. Acta Biomembr.*, 2009, **1788**, 1582–1592.
22 G. E. Boer, S. M. Hickey, A. G. Elliott and F. M. Pfeffer, *Eur. J. Med. Chem. Rep.*, 2022, **6**, 100089.
23 S. M. Hickey, T. D. Ashton, J. M. White, J. Li, R. L. Nation, H. Y. Yu, A. G. Elliott, M. S. Butler, J. X. Huang, M. A. Cooper and F. M. Pfeffer, *RSC Adv.*, 2015, **5**, 28582–28596.
24 S. M. Hickey, T. D. Ashton, S. K. Khosa, R. N. Robson, J. M. White, J. Li, R. L. Nation, H. Y. Yu, A. G. Elliott, M. S. Butler, J. X. Huang, M. A. Cooper and F. M. Pfeffer, *Org. Biomol. Chem.*, 2015, **13**, 6225–6241.
25 S. Dinesh Kumar, J. H. Park, H. S. Kim, C. D. Seo, C. Ajish, E. Y. Kim, H. S. Lim and S. Y. Shin, *Eur. J. Med. Chem.*, 2022, **243**, 114747.
26 P. Teng, H. Shao, B. Huang, J. Xie, S. Cui, K. Wang and J. Cai, *J. Med. Chem.*, 2023, **66**, 2211–2234.
27 R. S. Cheke, H. M. Patel, V. M. Patil, I. A. Ansari, J. P. Ambhore, S. D. Shinde, A. Kadri, M. Snoussi, M. Adnan, P. S. Kharkar, V. R. Pasupuleti and P. K. Deshmukh, *Antibiotics*, 2022, **11**, 566.
28 Q. Tang, H. Zhang, K. Chandarajoti, Z. Jiao, L. Nie, S. Lv, J. Zuo, W. Zhou and X. Han, *RSC Med. Chem.*, 2025, **16**, 1223–1234.
29 C. Ergene, K. Yasuhara and E. F. Palermo, *Polym. Chem.*, 2018, **9**, 2407–2427.
30 H. P. Rahn, X. Liu, M. B. Chosy, J. Sun, L. Cegelski and P. A. Wender, *J. Am. Chem. Soc.*, 2024, **146**, 22541–22552.
31 Y. Takada, H. Itoh, A. Paudel, S. Panthee, H. Hamamoto, K. Sekimizu and M. Inoue, *Nat. Commun.*, 2020, **11**, 4935.
32 E. van Groesen, P. Innocenti and N. I. Martin, *ACS Infect. Dis.*, 2022, **8**, 1381–1407.
33 M. P. Mingeot-Leclercq and J. L. Décout, *MedChemComm*, 2016, **7**, 586–611.
34 S. M. Hickey, T. D. Ashton, G. Boer, C. A. Bader, M. Thomas, A. G. Elliott, C. Schmuck, H. Y. Yu, J. Li, R. L. Nation, M. A. Cooper, S. E. Plush, D. A. Brooks and F. M. Pfeffer, *Eur. J. Med. Chem.*, 2018, **160**, 9–22.
35 K. Kuroda, G. A. Caputo and W. F. DeGrado, *Chem.–Eur. J.*, 2009, **15**, 1123–1133.
36 F. Devínsky, A. Kopecka-Leitmanová, F. Šeršeň and P. Balgavý, *J. Pharm. Pharmacol.*, 1990, **42**, 790–794.
37 Y. N. Albayaty, N. Thomas, M. Jambhrunkar, M. Al-Hawwas, A. Kral, C. R. Thorn and C. A. Prestidge, *Int. J. Pharm.*, 2019, **566**, 329–341.
38 K. Belfield, R. Bayston, N. Hajduk, G. Levell, J. P. Birchall and M. Daniel, *J. Antimicrob. Chemother.*, 2017, **72**, 2531–2538.
39 J. Li, Y. Suo, X. Liao, J. Ahn, D. Liu, S. Chen, X. Ye and T. Ding, *Ultrason. Sonochem.*, 2017, **39**, 101–110.